Redox Biology 21 (2019) 101108

Contents lists available at ScienceDirect

Redox Biology

journal homepage: www.elsevier.com/locate/redox

Non-enzymatic cleavage of Hsp90 by oxidative stress leads to actin aggregate formation: A novel gain-of-function mechanism

José Pedro Castro[a,b,d,e], Raquel Fernando[a], Sandra Reeg[a], Walter Meinl[a], Henrique Almeida[d,e], Tilman Grune[a,b,c,f,*]

[a] Department of Molecular Toxicology, German Institute of Human Nutrition, Potsdam-Rehbrücke, 14558 Nuthetal, Germany
[b] German Center for Diabetes Research (DZD), 85764 München-Neuherberg, Germany
[c] DZHK (German Centre for Cardiovascular Research), Partner site Berlin, 10117 Berlin, Germany
[d] Faculty of Medicine, Department for Biomedicine, University of Porto, 4200-319, Portugal
[e] Institute for Innovation and Health Research (I3S), Aging and Stress Group, R. Alfredo Allen, 4200-135 Porto, Portugal
[f] Institute of Nutritional Science, University of Potsdam, Nuthetal, Germany

ARTICLE INFO

Keywords:
Oxidative stress
Protein oxidation
Heat shock protein 90
Proteasome
Protein aggregates

ABSTRACT

Aging is accompanied by the accumulation of oxidized proteins. To remove them, cells employ the proteasomal and autophagy-lysosomal systems; however, if the clearance rate is inferior to its formation, protein aggregates form as a hallmark of proteostasis loss. In cells, during stress conditions, actin aggregates accumulate leading to impaired proliferation and reduced proteasomal activity, as observed in cellular senescence. The heat shock protein 90 (Hsp90) is a molecular chaperone that binds and protects the proteasome from oxidative inactivation. We hypothesized that in oxidative stress conditions a malfunction of Hsp90 occurs resulting in the aforementioned protein aggregates.

Here, we demonstrate that upon oxidative stress Hsp90 loses its function in a highly specific non-enzymatic iron-catalyzed oxidation event and its breakdown product, a cleaved form of Hsp90 (Hsp90cl), acquires a new function in mediating the accumulation of actin aggregates. Moreover, the prevention of Hsp90 cleavage reduces oxidized actin accumulation, whereas transfection of the cleaved form of Hsp90 leads to an enhanced accumulation of oxidized actin.

This indicates a clear role of the Hsp90cl in the aggregation of oxidized proteins.

1. Introduction

Functional disability associated to aging has been attributed to stochastic, genetic and environmental processes that lead to damage accumulation in cells and tissues [1–3]. While the underlying cause is debated, there is evidence favoring the processes of continued biological oxidation that, through the generation of by-products as reactive oxygen species (ROS) impinge on biomolecules, including proteins.

An important hallmark of oxidative conditions is protein carbonylation, a non-enzymatic chemical modification that is frequently observed in aged cells and tissues [4] which results in an irreversible protein structural modification and functional loss [5]. Mildly carbonylated soluble proteins are recycled by the proteasome. This multicatalytic enzyme assembles mainly in two forms, the ATP and ubiquitin independent 20S proteasome and the ATP and ubiquitin dependent 26S proteasome. Both have in common a cylinder-shaped structure resulting from the apposition of αββα subunit rings containing specific subunits; as the catalytic activity is exerted by some of the β subunits, the side positioning of α subunits limits the catalytic area exposure to hazards. While both forms of the proteasome are able to destroy and recycle proteins, it is the 20S proteasome that has been shown to be the main destination of oxidized or otherwise damaged proteins [6–12]; in turn, the 26S proteasome is able to degrade naturally folded and even functional proteins, if they are ubiquitin tagged [13].

Therefore, as long as the proteasome clears oxidized proteins from the cytoplasm, their accumulation is prevented. Eventually, as enhanced oxidation continues, proteasomal capacity is exceeded, protein destruction decreases and further oxidation is fostered. These events promote protein unfolding, hydrophobic residues exposure and the establishment of oxidized protein cross-links that result in insoluble,

* Correspondence to: Department of Molecular Toxicology, German Institute of Human Nutrition Potsdam-Rehbruecke (DIfE), Arthur-Scheunert-Allee 114-116, 14558 Nuthetal, Germany.
E-mail address: scientific.director@dife.de (T. Grune).

https://doi.org/10.1016/j.redox.2019.101108
Received 16 December 2018; Received in revised form 4 January 2019; Accepted 10 January 2019
Available online 11 January 2019

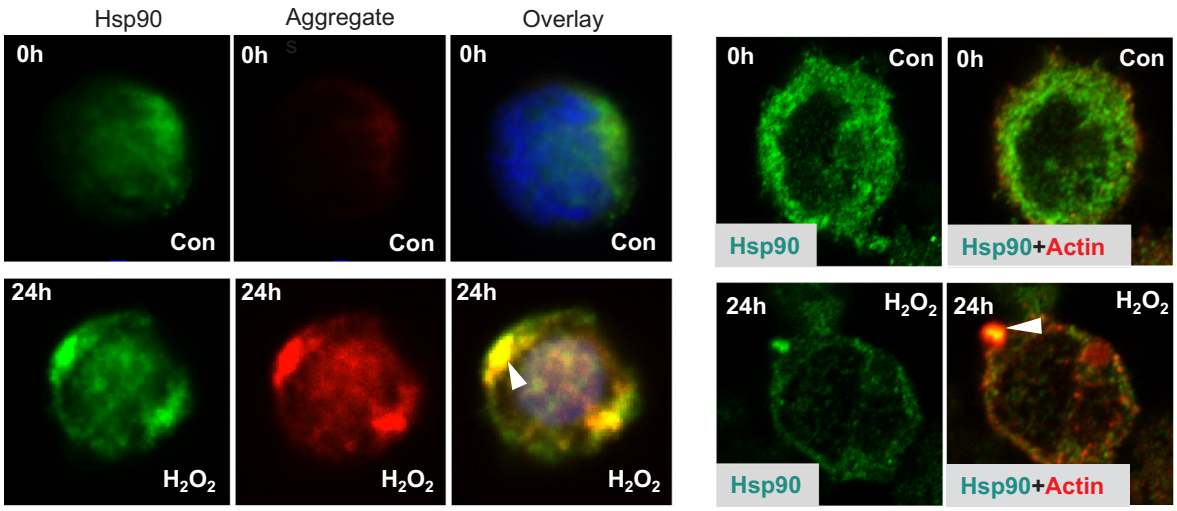

Fig. 1. Hsp90 accumulates in actin containing protein aggregates under oxidative conditions. In a previous report [27] we have shown that submitting Jurkat cells to 100 μM hydrogen peroxide for 24 h results in the formation of insoluble actin aggregates. The conditions were repeated and compared to 0 h exposure controls. **(A)** At 24 h of stress, fluorescence detection of Hsp90 protein (green labeling) and cell aggregate (red labeling) revealed a remarkable co-localization, not seen at 0 h. The nucleus was stained with DAPI (blue labeling) **(B)** Hsp90 accumulates in actin aggregates as evidenced by confocal microscopy detection of Hsp90 (green) and actin (red). While Hsp90 exhibits a fairly homogeneous, cell-wide distribution, actin is mostly localized to the periphery, near the cell membrane (left panels). Upon 24 h of hydrogen peroxide use, Hsp90 and actin co-localize and frequently exhibit aggregates (arrows at right panels).

high molecular weight aggregates that directly impair the ubiquitin-proteasome system [14], disturb cell functioning, and may cause cell senescence or apoptosis [15–17]. Protein aggregate accumulation thus reflects cellular proteostasis impairment and proteasome dysfunction; ultimately, it accompanies the aging process and conduces to organism disorder [18].

The mechanisms whereby oxidized proteins are delivered to the proteasome have remained elusive, but its elucidation would be of utmost importance for the understanding of cell functioning under various stress conditions. It was to suggested that there is a 'transporter-like' structure having a strong interaction with the oxidized protein and the 20S proteasome, their major destruction site. While Hsp70 was recently proposed to fulfil that function [19], the process was also described for the cytosolic protein calmodulin that, when oxidized by hydrogen peroxide, is delivered for destruction at the 20S proteasome in a selective interaction with the heat shock protein 90 (Hsp90) chaperone [20].

Hsp90 functions as a homodimer, whose monomers are composed of three distinct domains. The N-terminal domain promotes ATP hydrolysis required for chaperone substrate remodeling, the middle domain has a role in substrate binding and the C-terminal interacts with the other Hsp90 monomer and binds co-chaperones by the use of a TRP binding segment [21]. As a chaperone, Hsp90 assists a large number of native (client) proteins, mostly transcription factors and kinases, to fold properly into and hold their functional conformation [21]. So, Hsp90 interacts with pre-folded, configured proteins to assist them in stabilization of ligand binding regions, which frequently exhibit hydrophilic surface motifs [22]. Not surprisingly, Hsp90 inhibition is followed by client protein unfolding and ubiquitin tagging for destruction [21].

Interestingly, Hsp90 also interacts with the 20S proteasome, as reflected in the unusual difficulty in separating them [23]. In particular, Hsp90 binds to the proteasome α subunits [24] that, in the setting of oxidation, assists client protein degradation by the proteasome [20]. Moreover, such α subunit interaction appears to afford protection to the deeply located beta type, catalytic subunits; in fact, Hsp90 silencing in conditions of metal catalyzed oxidation, results in proteasome marked functional decline and even inactivation [25,26].

In a previous study, we have verified that submitting a T cell line to hydrogen peroxide mediated oxidative stress resulted in proteasome inhibition, oxidized protein aggregates formation and cell proliferation arrest [27], characteristic features of aged and senescent T cells *in vivo* [28,29] and *in vitro* [30]. Furthermore, under the same conditions, actin was found as most susceptible to oxidation and prone to aggregate formation [27]. Interestingly, in a lymphocyte cell line [31] and skeletal muscle extracts [32] functional Hsp90 was found to bind actin, to establish crosslinks with its filaments [31] and to promote bundle formation [21]. In contrast, Hsp90 inhibition resulted in actin polymerization [33] further emphasizing Hsp90 importance in actin functioning. As actin has been considered a client protein of Hsp90 chaperone activity [31–37], it is possible that a peculiar hydrophobic cleft with relevance for actin filament growth [38] is the structural feature that provides support for Hsp90 interaction.

We hypothesized that under conditions of oxidative stress, the physiological interaction between Hsp90 and actin is impaired and the damaged actin has a fate similar to that described earlier of calmodulin.

Therefore, we investigated the role of Hsp90 function in proteostasis following oxidative stress. Interestingly, a new function of an Hsp90 form, the Hsp90 cleaved (Hsp90cl), was discovered. This gain-of-function mechanism presents, to our knowledge, a novel mechanism for protein aggregate formation, which might be important in revealing the mechanism of age-depended protein aggregate formation.

2. Results

2.1. Hsp90 accumulates in protein aggregates upon oxidative stress and associates with actin

In Jurkat cells submitted to a 24 h hydrogen peroxide mediated-oxidative stress, there is a decrease in proteasome activity at 3 h and 24 h (Fig. S1); this last observation had been reported before [27] and interpreted as consequence of the accumulation of cytoplasmatic aggregates containing carbonylated actin [27]. As these findings

commonly accompany the increase in protein unfolding or misfolding and proteostasis impairment [39–41], it was reasoned that oxidized actin accumulation was the consequence of reduced proteasome ability ([Fig. S1] and [27]) and disturbed actin interaction with Hsp90. Therefore, we analyzed protein aggregates containing cells, which are well formed after exposing them to stress for 24 h [Fig. 1 [27],] for the presence of Hsp90. Interestingly, Hsp90 could be co-localized with protein aggregates (Fig. 1A) containing actin (Fig. 1B). In fact, while without stress a uniform cytoplasmic display of Hsp90 and only peripheral concentration of actin was noticed (Fig. 1B [27]) after 24 h of stress, Hsp90 labeling was evidenced as condensed masses, with a distribution that co-localized to actin aggregates (Fig. 1B, bottom).

2.2. Hsp90 is cleaved after oxidative stress into a smaller fragment in an iron dependent process

Having noticed the proximity of actin aggregates to Hsp90 under stress conditions, the early hypothesis of Hsp90 functional disturbance could be confirmed. Since, it is known that oxidative stress might change chaperone expression; we performed immunoblots to confirm Hsp90 amounts. However, there was a notorious decrease in the Hsp90 90 kDa band at 24 h after oxidative stress, compared to 0 h (Fig. 2A). Interestingly, instead of a single Hsp90 band, a second band ~ 70 kDa was detected. While a dramatic expression of an Hsp90 inducible form was unlikely, as its molecular weight would be larger, the most probable effect was Hsp90 cleavage, similarly to previous reports showing the appearance of a 73 kDa band upon Hsp90 cleavage at its N-terminal extremity [42,43]. Moreover, we followed the cleaved form (Hsp90cl) over time and found that it was maintained up to at least 96 h, and this was associated with cellular proliferation inhibition (Fig. S2). To confirm, an Hsp90 N-terminal detecting antibody was employed, anticipating that no 73 kDa band would be evidenced at 24 h. Thus, 100 μM H_2O_2 treated cells extracts were reacted with antibodies against Hsp90 full length and N-terminal segment. As expected the full length antibody detected a double band at 84 and 73 kDa (Fig. 2B, left panel) but only the heavier 84 kDa band was visualized if the N-terminal was employed instead (Fig. 2B, middle panel). Since iron was considered a co-factor for Hsp90 cleavage and the formation of the 73 kDa Hsp90cl [43], DFO (deferoxamine) was used to deplete iron from cells, before submitting them to oxidative stress. As expected, in cells not subjected to DFO, there was Hsp90 cleavage as evidenced by the double band (Fig. 2C, left lane); in contrast, in DFO-treated, iron-depleted cells, there was a single band showing that Hsp90cl had not been formed (Fig. 2C, right lane), thus indicating that the process is iron dependent. Moreover, employing a cell-free system with purified recombinant Hsp90, it was shown that Hsp90 cleavage is non-enzymatic (Fig. 2D) and dependent on Fenton reaction to occur as previously reported [43].

Therefore, these data demonstrate that oxidative stress conditions cause Hsp90 cleavage into a 73 kDa Hsp90cl protein, by a non-enzymatic, iron-dependent process.

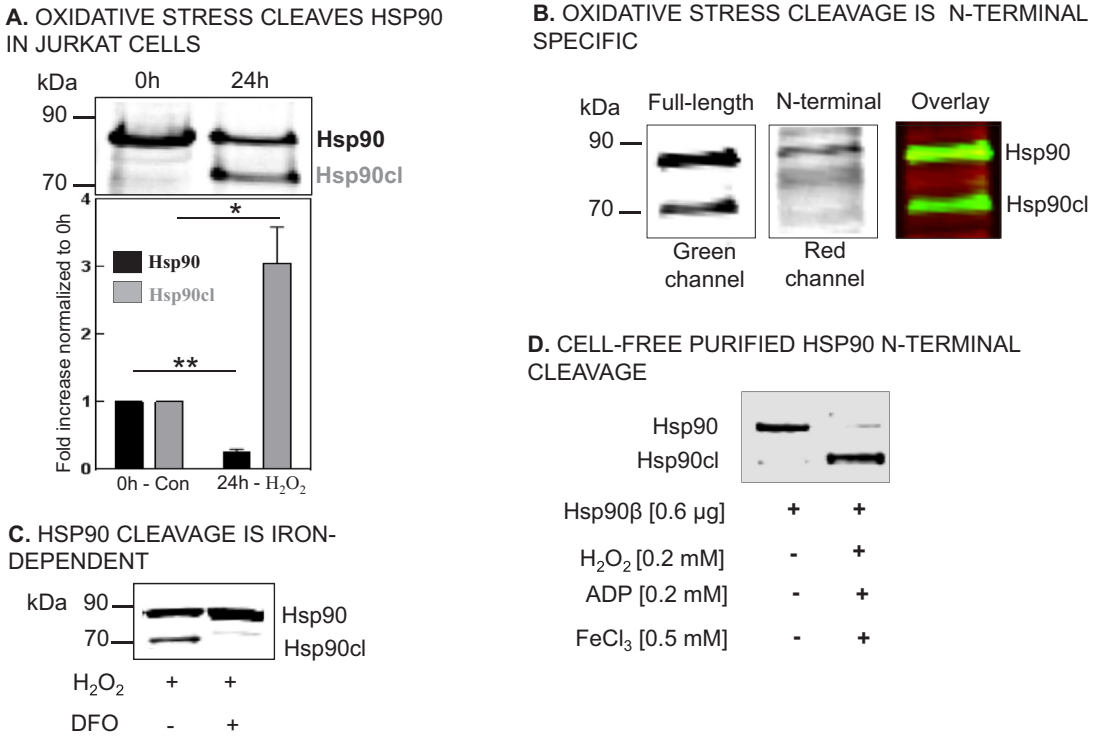

Fig. 2. Oxidative stress promotes Hsp90 chaperone cleavage into a 73 kDa form (Hsp90cl) dependent in an iron-catalized oxidation. (A) Jurkat cells were exposed to 100 μM hydrogen peroxide for 24 h and compared to controls (0 h exposure). Immunoblots were prepared with antibodies against Hsp90 (top image), and band densitometry was quantified (bottom chart). Upon 24 h exposure, Hsp90 level decreased ~ 50% and a new 73 kDa band appeared, consequent to Hsp90 N-terminal cleavage, identified as Hsp90cl. Quantification of Hsp90 and Hsp90cl is the result of three independent experiments (Mean ± standard deviation SD, *t*-test *$p < 0.05$, **$p < 0.01$). **(B)** Extracts of Jurkat cells submitted to 100 μM hydrogen peroxide for 24 h were immunoblotted employing Hsp90 full length and Hsp90 N-terminal specific antibodies. Detection was made with secondary antibodies bearing different fluorochromes. Full length antibody detected two bands [as in (A)], whereas the N-terminal antibody reacted only with the full length Hsp90 (84 kDa band), indicating that Hsp90cl band resulted from N-terminal Hsp90 cleavage. Overlay signal co-localizes only in the 84 kDa band, thus showing that the 73 kDa protein lacks the N-terminal fraction. Membrane fluorescence was detected with Li-Cor Odyssey. (C) Iron is required for Hsp90 cleavage. Cells depleted in iron upon DFO use do not exhibit Hsp90cl even when exposed to hydrogen peroxide for 24 h (right lane). In contrast, exposed cells without iron depletion, showed the expected double band pattern (left lane). (D) Hsp90 cleavage in a cell free system. Recombinant Hsp90β (constitutive) was subjected to hydrogen peroxide (0.2 mM) in the presence of ADP and $FeCl_3$. Oxidant dependent cleavage into Hsp90cl was detected.

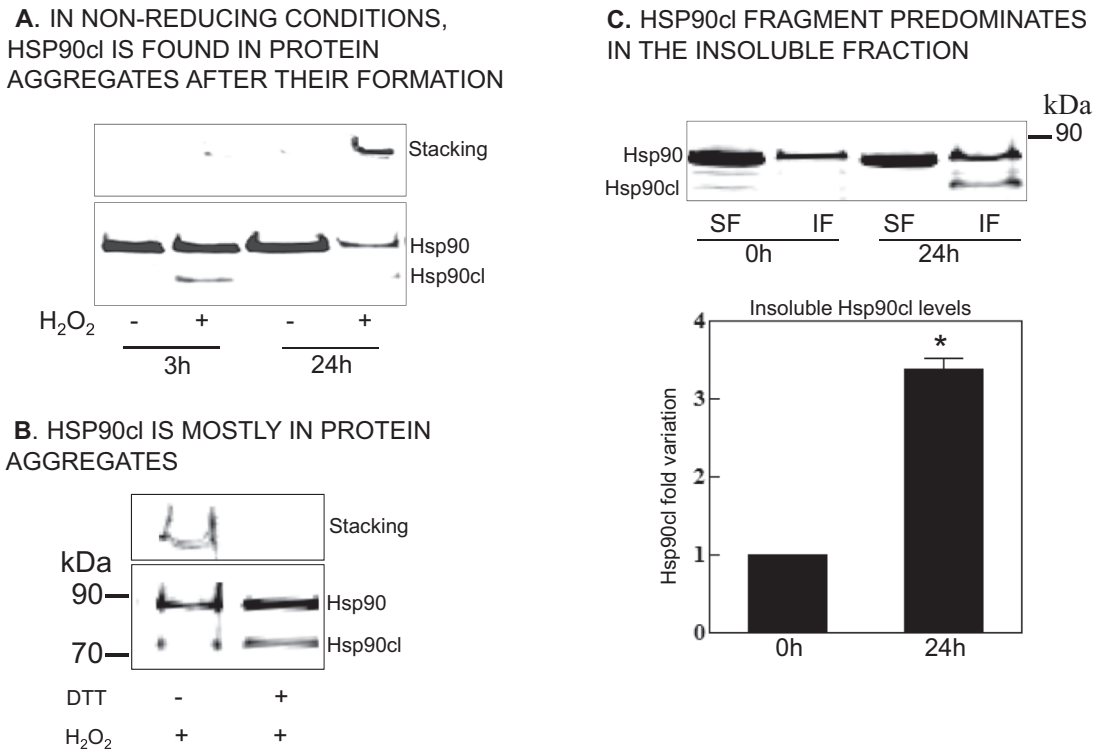

Fig. 3. Hsp90cl accumulates as insoluble aggregates. (A) In an PAGE with non-reducing conditions, aggregates can be seen after 24 h of oxidative stress, but not at time points as early as 3 h. Interestingly, Hsp90cl form is visualized after an oxidative stress short-term insult and appears to be re-localized to the stacking gel after 24 h, where Hsp90cl-positive aggregates can be observed. **(B)** Hsp90cl is present in aggregates. Upon Jurkat cells exposed to 100 μM hydrogen peroxide in a medium without or with the aggregate dissolving agent DTT, Western blots were probed with the full length anti Hsp90 antibody. In conditions without DTT, a band is retained at the stacking gel and the 73KDa protein is faint or missing (left lane); when DTT is added, aggregates dissolve and migrate into the separating gel (right lane), where they exhibit the 84 kDa and the 73 kDa bands, indicating that the Hsp90cl was previously retained in aggregates and now migrated into the stacking gel. The blot is a representative of 3 different experiments. **(C)** Hsp90cl is localized to the insoluble fraction. Jurkat cells were exposed to 100 μM hydrogen peroxide for 24 h and compared to controls (0 h exposure). Total protein extracts samples from time-point 0 h and 24 h of oxidative challenge were separated as soluble (SF) and as insoluble (IF) fractions. Hsp90cl shows a 3-fold content increase in the insoluble fraction upon oxidative stress (lower chart) supporting the view that Hsp90cl is localized mainly in protein aggregates. The blot is representative of 3 different experiments (Mean ± SD are shown, *t*-test *p < 0.05).

2.3. Cleaved Hsp90 accumulates as insoluble protein aggregates

The existence of two forms of Hsp90 raises the question of their roles and which form of Hsp90 is accumulating in actin aggregates. Earlier studies (unpublished data) demonstrated that actin aggregates are unstable under strong reducing conditions. Therefore, under non-reducing conditions, we tested for the presence of Hsp90cl in protein aggregates after 24 h of oxidative stress, known to be enough time for cells to form actin aggregates. In addition, we analyzed cell lysates at a 3 h stress time-point, when aggregates are not formed yet. As can be clearly observed in non-reducing conditions, Hsp90 cleavage occurs at earlier time points, but the protein is not detected in the stacking gel (Fig. 3A); however, at 24 h of oxidative stress, Hsp90cl was no longer detected at the expected position, but a new band was notorious in the stacking zone of the blot, suggesting Hsp90cl presence in protein aggregates (Fig. 3A). To explore further this point, we tested the presence of Hsp90cl in protein aggregates under non-reducing as well as reducing conditions after 24 h of hydrogen peroxide treatment. In this test, while non-reducing conditions replicated the previous experiment and did not evidence the 73 kDa protein but did show protein bands at the stacking gel, the use of DTT reversed these findings: it restored the Hsp90cl band at 73 kDa but did not show any bands at the stacking zone of the gel (Fig. 3B). It thus indicated that a major fraction of the Hsp90cl is located within the protein aggregates.

To further confirm this finding, and because protein aggregates are known to become insoluble, we separated the protein extracts into, soluble (SF) and insoluble (IF) fractions and assessed for cleaved Hsp90cl. Quantification in the IF at 24 h of stress revealed a > 3 fold increase of Hsp90cl compared to untreated cells (Fig. 3C, lower chart), thus providing strong evidence that upon oxidative stress, the formed Hsp90cl accumulates in aggregates as insoluble material. Interestingly, after silver staining of the gel, followed by excision of the band from the stacking gel and mass spectrometry analysis, actin was identified with a Protein Score and a Confidence Interval of about 98% (Fig. S3). These set of results confirm Hsp90cl and actin interaction in oxidative stress induced-protein aggregates.

2.4. Hsp90 cleavage antedates actin accumulation

As Hsp90 plays an important role in oxidized protein degradation and in 20S proteasome protection [20,26], we found that a cleaved Hsp90cl does not prevent oxidized proteins, as cytoplasmic actin, to accumulate. To test that, a temporal assessment was made at 0 h, 3 h, 6 h and 9 h to verify actin and Hsp90 abundance in soluble (SF) and insoluble (IF) fractions. As depicted in Fig. 4A, at each time point, actin is more abundant in SFs but accumulation in the IF starts at 6 h or 9 h time-point and continues afterwards (Fig. 4A and C). As to Hsp90cl, its residual presence at 0 h is probably due to the high ROS production by cultivated cells [44–46]; however, later at 3 h time-point, there is strong cleavage enhancement (Fig. 4B and Fig. 3A) and, from 6 h onwards, Hsp90cl shifts from SF to IF (Fig. 4A and C).

While at 24 h of stress, actin aggregates accumulate and the proteasome function is impaired [27], at 3 h such changes are slight, a difference that is probably related to the amount of oxidative burden imposed and not due to aggregates. In fact, a mild oxidation of actin and particularly its association with Hsp90 is useful for proteasomal

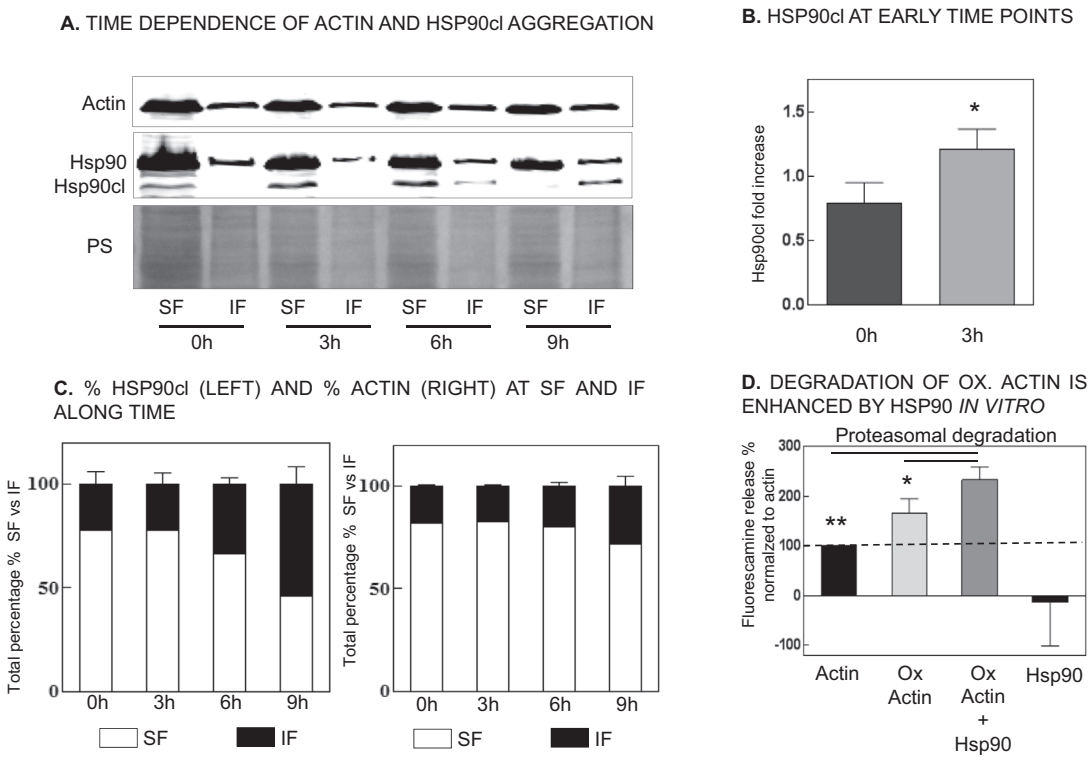

Fig. 4. Oxidative stress related Hsp90cl appearance is time-dependent and localizes in the cytoplasmic insoluble fraction. Upon cell exposure to 100 μM hydrogen peroxide, samples were collected at 3 h, 6 h, and 9 h and compared to controls (0 h). **(A)** Extracts from controls and treated cells were prepared for separation of soluble and insoluble fractions. Oxidative conditions promote Hsp90 cleavage, already evident at 3 h. Hsp90cl form remains in the cytoplasmic soluble fraction until 6 h, when it shifts towards insolubility, which is notorious at 9 h post stress. Ponceau S staining (PS, bottom image) and western blots with antibodies against full length Hsp90 (middle image) and actin (top image) are depicted in this representative image. **(B)** Quantification of Hsp90cl at the soluble fraction confirms that it is already enhanced at 3 h. **(C)** Quantification of relative % of actin (right graph) and Hsp90cl (left graph) in soluble (SF) and insoluble (IF) fractions. Actin level increases in the insoluble fraction, after time point 6 h, when Hsp90cl had already accumulated considerably and when aggregate formation is likely to begin. It thus indicates that Hsp90 cleavage and accumulation at the IF precedes actin aggregate accumulation. Graphic bars result from three independent experiments (Mean ± SD are shown). **(D)** Hsp90 enhances proteasomal degradation *in vitro*. In a cell free system, proteasomal degradation of actin/oxidized actin was measured after adding to the medium actin, oxidized actin, oxidized actin plus Hsp90 and Hsp90 only. Activity was normalized to 100% in the condition of actin only and compared. Oxidized actin is degraded about 1.6fold better than non-oxidized. However, the degradation of oxidized actin is further enhanced to an 2.4fold increase in the presence of Hsp90. Graphic bars result from three independent experiments (Mean ± SD are shown, *t*-test *p < 0.05, **p < 0.01, each compared to ox actin + Hsp90).

degradation of the mildly oxidized actin, suggesting that such an association is beneficial for protein degradation at the proteasome (Fig. 4D).

2.5. Cleaved Hsp90 directly leads to the formation of actin aggregates

In order to confirm that the cleaved form of Hsp90 was directly responsible for the aggregate formation, we set up a purified *in vitro* model with oxidized actin, the 20S proteasome and with Hsp90 or Hsp90cl. As depicted in Fig. 5A, co-incubation of Hsp90cl, oxidized actin and 20S proteasome resulted in protein aggregate formation (stacking gel, arrows), possibly due to the lesser ability of Hsp90cl to deliver oxidized actin to the 20S proteasome (left blot). Moreover, actin was also detected in the stacking gel when Hsp90cl was present, supporting its gain-of-function role as (actin) aggregate promoter. In contrast, co-incubating Hsp90 with oxidized actin and 20S proteasome likely culminated in oxidized actin degradation, explaining why no aggregates were found in the stacking zone of the blot when probing against Hsp90 or actin.

To prove that it is the cleaved Hsp90 that directly promotes protein aggregates in a complex system, we decided to overexpress it in cells. In the beginning, a plasmid with the known sequence for Hsp90cl [43] was constructed, interestingly without the N-terminus, the protein could not be expressed because of impaired translation or immediate degradation (data not shown). To overcome this problem, a different plasmid was constructed, where sequences of Ypet and a flexible linker were inserted to mimic the N-terminal and avoid non-translation or degradation. The protein could now be overexpressed [Fig. S4 and S5 and [47]] as well as Hsp90cl.

To confirm our hypothesis we performed immunoblots against both Hsp90 and actin in order to make sure that under oxidative stress and Hsp90cl overexpression more aggregates would form. Observing the stacking zone of the blot (Fig. 5B, upper panel) it can clearly be seen that more protein aggregates are formed under oxidative stress when Hsp90cl is overexpressed, confirming that the Hsp90 fragment is the most important factor for the accumulation of protein aggregates. When hydrogen peroxide was added most of the cleaved overexpressed form (Hsp90cl + Ypet, approx. 100 kDa) is in aggregates at the stacking gel, because a decrease could be detected in the normal weight band of Hsp90 + Ypet when using H_2O_2, in contrast to non-stress conditions.

Moreover, to visualize actin aggregates display in cells, using the same experimental conditions as above (Fig. 5B), we co-transfected cells with Actin-GFP plasmids, enabling us to follow protein (actin) aggregate formation. As can be observed from confocal microscopy image analysis (Fig. 5B, bottom panel), upon oxidative stress and Hsp90cl overexpression, actin-GFP was found to form large well-defined aggregates in clear contrast when comparing to oxidative stress condition solely or when Hsp90f overexpression was added (only non- or residual-condensed actin-GFP spots were found). These set of results remarkably demonstrate that Hsp90 upon cleavage promotes protein

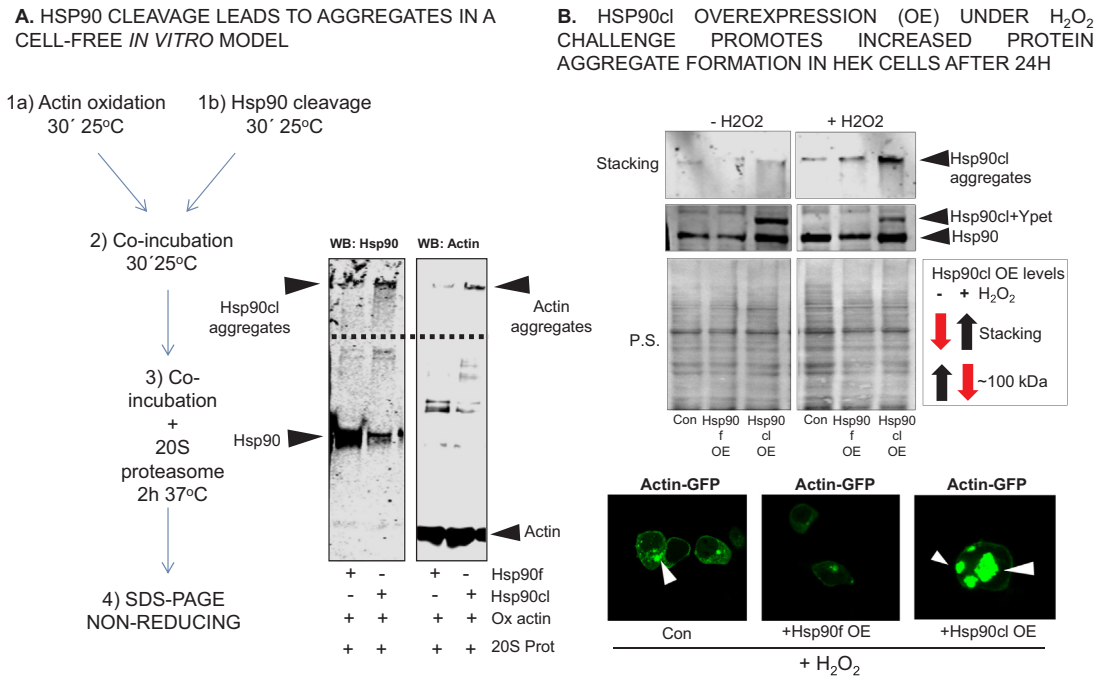

Fig. 5. A new gain-of-function of Hsp90cl leads to the formation of protein aggregates. (A) In a cell-free purified *in vitro* model, Hsp90f or Hsp90cl were co-incubated with oxidized actin for 30 min at 25 °C; then, purified 20S proteasome was added to the mix for 2 h at 37 °C to allow 20S proteasome enzymatic activity. The immunoblots were performed under non-reducing conditions (without DTT) therefore showing protein aggregates in the stacking zone (above the dotted line. Hsp90 antibodies (left blot) and anti-actin antibodies (right blot) were used. Whereas by using the Hsp90cl form aggregates could be detected, in controls where oxidized actin and 20S proteasome were co-incubated with full-length Hsp90, aggregates were not found. **(B)** HEK cells were used to overexpress Hsp90 (Hsp90f OE) and Hsp90cl-Ypet (Hsp90cl OE). The upper panel depicts a Western blot against Hsp90 showing that Hsp90cl overexpression under oxidative stress leads to an enhanced protein aggregate formation comparing to other conditions where H_2O_2 was also employed (stacking). Stacking and separating gels were analyzed with anti-Hsp90 antibodies or stained for protein (P.S.). Bottom panel – Confocal microscopy confirmation using actin-GFP transfected cells to demonstrate the role of Hsp90cl in actin aggregate formation under oxidative stress.

aggregates formation in a new gain-of-function mechanism.

3. Discussion

In the course of cellular metabolism, oxygen use generates a variety of by-products that include the reactive oxygen species whose continued production subjects biomolecules to harmful, oxidant effect [48]. The appearance of irreversibly affected molecules has been considered a mark of oxidative stress and their accumulation in the last third of organism´s life [4] is evidence in favor of the importance of oxidation for aging.

In cells, adding to functional impairment, oxidation results in protein structural abnormalities as unfolding. Consequently, usually buried hydrophobic domains become exposed and promote the establishment of cross-links with other oxidized proteins, which antedate the formation of insoluble protein aggregates [49]. These findings, apart from being consequence of a continued or intense oxidative environment, are features of aged cells, able to interfere with their metabolism, cause changes in gene expression and lead to their senescence or death. Aggregates have been correlated with aging progression across different models such as bacteria [50,51], yeast [52], *C. elegans* [53] and mammalian cells [54].

The appearance of abnormal or no longer necessary proteins triggers a disposable mechanism that directs them for destruction at the 26S proteasome upon tagging by ubiquitin molecules. Yet, in the case that proteins are mildly oxidized, they may be directed through an additional, different process that targets them to the 20S proteasome, also aiming at cell homeostasis maintenance and cross-linked protein accumulation prevention [9,55,56]. In fact, the 20S proteasome was considered the main system involved in the degradation of oxidized proteins [26]. Among others, in the case of calmodulin [20,57] and actin (current study), there is evidence that oxidized proteins, compared to native proteins, are degraded by the proteasome at a higher rate. The primary nature of chemical changes undergone by both molecules emphasizes further similarity as it is the Sulphur containing methionine residues in calmodulin [20] and specific cysteine and methionine residues of actin [58,59] that are sensitive to the early oxidative modification.

Oxidized proteins tagged for destruction require the interaction with chaperones before they are transported to the proteasome. In this setting, the Hsp90 chaperone protein is an important cellular tool when proteostasis is challenged due to its cytoplasmic abundance and ability to interact with a vast number of proteins [21]. In particular, Hsp90 is known to bind strongly to actin [31,32] and calmodulin [20]. In addition, the Hsp90 ability to enhance their degradation at the proteasome, shown before [20] and in the current study, favors its involvement in their transportation. Hsp90, indeed, was recognized as an active intracellular chaperone when cells are affected by carbonylation [60].

When the oxidative insult is intense, actin aggregates are formed as reported before [27,59] and in the current study. Although they associate with the Hsp90 molecule, it is a 73 kDa fragment, the Hsp90cl, that becomes an important component of the aggregate, as shown in the present study; such cleavage is not unexpected as oxidative stress impinges on amino acid residues and may cause polypeptide backbone fragmentation [61]. In the case of Hsp90, the cleavage is detectable in intact cells, their lysates and purified recombinant proteins and it is a consequence of a non-enzymatic process requiring iron; this is thought to be chelated and cause Hsp90 cleavage at an highly conserved N-terminal amino acid motif following a local Fenton reaction [43]. The consequences are loss of ATP binding domain and impairment of Hsp90 chaperoning function [43], although the authors did not assess actin's

fate and possible protein aggregate formation.

Moreover, the oxidative stress related Hsp90 functional loss is likely to contribute to the observed proteasome derangement. In fact, in the current model of oxidative stress on Jurkat cells, proteasome activity reduction was reported as early as 3 h and had intensified at 24 h (current study and [27]). In another report, Hsp90 silencing was found to account to reduced proteasome trypsin-like activity and Hsp90 overexpression was able to maintain the level of proteasome activity in harsh oxidizing conditions, suggesting a proteasome protective effect [25,26]. Therefore, these observations, in agreement with previous findings [9,14,56], provide ample evidence that oxidative conditions impair proteasome activity.

So, the data indicate that while mildly oxidized, actin is perhaps in association with Hsp90 conveyed to the 20S proteasome for degradation, under too high or prolonged oxidative conditions the proteasome function becomes impaired, Hsp90 is cleaved and actin crosslink establishment is promoted. These events converge into a time-related, reduced availability of functional Hsp90 and enhanced conditions for actin insoluble cytoplasmic aggregates deposition. In fact, our *in vitro* cell-free assay using purified constituents such as oxidized actin, 20S proteasome and Hsp90 (full length) or Hsp90cl demonstrated that in presence of the latter, protein aggregates are formed. This finding supports the importance of a full functional Hsp90 to shuttle oxidized actin to the 20S proteasome for degradation. When this process is impaired, aggregates are formed, because oxidized actin fails to be degraded and accumulates together with Hsp90cl. Moreover, in a complex system as cells, we were able to demonstrate that Hsp90cl is the key player for protein aggregates formation, by Western blot and confocal microscopy.

Other features as proliferation arrest and reduced functional capacity of the proteasome observed in Jurkat cell line has a parallel with a previous report with primary T cells [28,29], whose changes were interpreted as consequent to immune cells aging. In fact, there is substantial evidence in favor of an age-related and cell senescence-related decrement in proteasome activity [62–65]. Indeed, many other authors have shown that Hsp's can be up-regulated upon stress conditions and inflammation [66]. The fact that this strongly correlates with the presence of an inflammatory condition suggests a relevant biological significance for this mechanism. Taking all into account we are convinced that early Hsp90 chaperoning ability loss upon cleavage and proteasome reduced functioning are among the prime events that lead to protein aggregates formation.

As a conclusion, we here show a novel mechanism for accumulation of oxidized proteins into protein aggregates. Unraveling how oxidized proteins clump together into protein aggregates is of utmost importance in the aging context. This study may provide the background knowledge to design approaches in order to prevent or delay the progressive accumulation of insoluble oxidized protein aggregates seen over time.

4. Methods

4.1. Cell culture

Jurkat cells were cultured in a medium containing RPMI 1640, with 10% FBS, 1% L-glutamine, 1% Penicillin/Streptomycin (Biochrom) at 37 °C, 5% CO2 in a NUAIRE™ US Autoflow CO_2 water-jacketed were submitted to oxidation by adding 100 μM hydrogen peroxide (H_2O_2, Sigma) for 3 h, 6 h, 9 h and 24 h and comparing to 0 h time-point. When employed, 500 μM Desferoxamine (*DFO*, Novartis) was used 18 h before exposure. HEK293 cells were cultured in Dulbecco's modified Eagle's medium (DMEM) supplemented with 10% fetal calf serum,1% L-alanyl-L-glutamine and 0.35% additional glucose, in an atmosphere of 5% CO_2 and 37 °C. HEK 293 cells were transfected with 1.5–2 μg pcDNA3.3 plasmid vector either with the cDNA sequence for Hsp90 full length or Hsp90 cleaved expression (please see *Hsp90 and Hsp90cl overexpression plasmids*). Co-transfections with Actin-GFP (1.5 μg), were performed with Lipofectamine 3000 (ThermoFisher Scientific, Schwerte,Germany) 24 h after seeding the cells. Afterwards, following the time of the transfections, 100 μM hydrogen peroxide (H_2O_2) was added to the cells for an extra period of 24 h.

4.2. Immunoblotting

For each experiment or time point, Jurkat and HEK293 cells were lysed in 0,1% TritonX-100, 20 mM NaCl, 30 mM Tris pH 7,4, 1 mM EDTA and 100 mM DTT (Lysis Buffer, LB), collected, briefly sonicated and protein quantified by the Bradford method [67]. A total of 10 μg of protein was heated at 65 °C for 30 min and samples were loaded and resolved in a 10–12% SDS-PAGE gel. Proteins were blotted onto nitrocellulose membranes (BioRad) and stained with Ponceau S for protein loading control. Next, membranes were blocked with 5% BSA/TBST (Tris Buffer Saline with Tween 20, 0.1%) for 1 h. When the experiment was designed to detect protein carbonylation, membranes were directly derivatized with 2,4-dinitrophenylhydrazine (DNPH, Sigma Aldrich). Briefly, after the transfer, membranes were equilibrated in TBS (Tris Buffer Saline)/20% Methanol, washed for 5 min in 10% Trifluoroacetic acid (TFA, VWR), incubated for 10 min with 5 mM DNPH/TFA (10%) in the dark, washed with TFA (10%) to remove DNPH excess and washed again five times (5 min each) with 50% methanol. They were then blocked with 5% BSA/TBST (Tris Buffer Saline with Tween 20, 0.1%) for 1 h. After blocking, the membranes were probed with rabbit anti-Hsp90 full length at a dilution of 1:7500 (Abcam), and mouse anti-actin (Santa Cruz) at a dilution of 1:2000, mouse anti-Hsp90 N-terminal at 1:1000 (Abcam) and a mouse HA-tag antibody (Abcam) at a dilution of 1:1000. For secondary antibodies, IRDye 800CW or IRDye 680LT were used at 1:20000 dilution, depending on primary antibody. They were purchased from Li-Cor Odyssey. The detection was performed at infrared, using the Li-Cor equipment from Odyssey. Band intensities were quantified by densitometry using Odyssey software. Graphics were made using GraphPad Prism 5 software.

4.3. Immunocytochemistry

Cells were grown on 6-well plates for 24 h, and after washing in PBS, they were placed in poly-L-Lysine slides (Jurkat T cell line are suspension cells) and allowed to dry in the incubator described above (see *Cell culture conditions*). Immediately after, they were fixed in 4% PFA (Para-formaldehyde), washed with PBS, PBST (Phosphate Buffer Saline with Tween 20 0.1%) and PBSTx (Phosphate Buffered Saline with Triton X 0.1%) 0.1% and incubated for one hour in PBST/BSA 2%, to lower unspecific background signal. Then, they were incubated overnight at 4 °C in a solution containing the diluted primary antibodies: 1:250 of goat anti-β-actin (Santa Cruz, USA) and 1:200 of rabbit anti-Hsp90 (full length). After washing twice in PBST, cells were incubated with the secondary antibodies conjugated with Alexa fluorochromes from Molecular Probes, donkey anti-goat secondary antibody conjugated with Alexa 488 and 568 (1:1000 prepared in PBST with 2% BSA) and with anti-rabbit secondary antibody conjugated with Alexa 488 and 568 (1:1000 prepared in PBST with 2% BSA) and donkey anti-mouse secondary antibody conjugated with Alexa 568 (Molecular Probes) 1:1000 prepared in PBST with 2% BSA). For aggregate detection and co-localization, a marker dye (Aggresome Detection Kit, Enzo Life Sciences) was prepared according to the manufacturer protocol. Fluorescence samples were analyzed on a fluorescence microscope Zeiss AxioImager Z1 in Porto, Portugal.

4.4. Confocal microscopy

Transfected HEK cells were grown (see conditions above) in glass bottom dishes Samples were then fixed in PFA 4% and washed in PBS for further investigation with a Zeiss *LSM780* confocal laser scanning

microscope at 40-fold magnification and scanned in high resolving *tile*-mode, maintaining non-overlapping images while recording most of the sample. Scanning was done in *best signal*-mode in order to avoid *spectral bleed-through*. Laser intensity and confocal plane thickness was the same for every condition.

4.5. Cellular fractioning

After several time-points control cells and 100 μM H_2O_2 treated cells were lysed in LB, and centrifuged at 21,100 g for 35 min 4 °C to separate soluble fraction (SF) from insoluble fraction (IF). Supernatants (SF) were collected, and pellets (IF) were resuspended in resolubilization buffer (7 M urea, 2 M thiourea, 4% CHAPS and 100 mM DTT, RB), adapting a previously described procedure [68].

4.6. In vitro Hsp90 cleavage and actin oxidation

In a tube, 0.6 μg recombinant human Hsp90β (Enzo Life Sciences) was subjected to 0.2 mM ADP and 0.5 mM $FeCl_3$ for 30 min at 25 °C, with mild agitation. Afterwards, 0.2 mM of H_2O_2 was added during 30 min at 25 °C in order to promote non-enzymatic cleavage. The reaction was stopped adding Gel Loading Buffer and 0.1 mM DTT. Samples were then loaded for SDS-PAGE, followed by immunoblot detection against Hsp90, as described above. Non-muscle actin (Cytoskeleton) oxidation was performed according to [27].

4.7. Proteasomal degradation of oxidized actin

Oxidized actin and controls (non-oxidized Actin and Hsp90β) were incubated with isolated 20S proteasome [57], and 2 μg of recombinant human Hsp90β were added, incubated for 2 h at 37 °C and later centrifuged for 10 min at 3000 g. To 125 μl of supernatant and 625 μl of 1 M HEPES, fluorescamine (Sigma Aldrich, 47614) solution was added for a final concentration of 0.03% and incubated for 5 min. Fluorescamine reacts with primary amines, leading to the formation of a fluorescent product measured at 390 nm excitation/475 nm emission wavelength. A series of dilutions of glycine (from 0.05 to 10 mM) were used as standard. Proteolysis rate was calculated as the difference between proteasome and blank samples (without addition of isolated 20S proteasome).

4.8. Proteasome activity measurement

Cells were counted, and the same number of cells was washed twice with PBS in each tube. Cells suspensions were centrifuged for 5 min at 30 g and lysis buffer (250 mM sucrose, 25 mM Hepes, 10 mM magnesium chloride, 1 mM EDTA, and 1.7 mM dithiothreitol (DTT)) was added to the pellet. Cells were lysed using a 20-gauge syringe, followed by repeated freeze–thaw cycles. Afterward, the cell lysates were centrifuged at 3500 g for 30 min and the supernatants were used for determination of proteasomal activity. Samples of the supernatants were incubated in 225 mM Tris buffer (pH 7.8), 45 mM potassium chloride, 7.5 mM magnesium acetate, 7.5 mM magnesium chloride, and 1 mM DTT. To measure chymotrypsin-like activity of the proteasome the fluorogenic peptide suc-LLVY-MCA was used as a substrate at a final concentration of 200 μM. Samples were incubated for 30 min at 37 °C. The proteolytic MCA liberation was measured using a fluorescence reader (Reader EL 340; Bio Tek Instruments, Bad Friedrichshall, Germany) at 360 nm excitation and 460 nm emission. Free MCA was used as the standard for quantification.

4.9. Plasmids and cloning strategy

The pcDNA3_EGFP_ß-actin plasmid was a generous gift from Beat A. Imhof, University of Geneva, Switzerland [69]. The pcDNA3_HSP90_HA plasmid was a gift from William Sessa (Addgene plasmid # 22487). This plasmid served as a template to generate an untagged as well as a hemagglutinin (HA) tagged reading frame of the cleaved HSP90. However neither of these cleaved forms expressed detectable amounts of protein, although the translational context was the same as in the well expressed HA-tagged full length HSP90 ORF. In order to get an expression of the cleaved HSP90 we therefore decided to fuse the HSP90 sequence after the Gly codon 127 with a not functional N-terminal domain consisting of the Ypet ORF [70] and a flexible linker (three times repeated Ser-Gly-Gly-Gly-Gly and a final Ser motif. The strategy was to replace in the original pcDNA3_HSP90_HA plasmid the sequences between a HindIII site in the C-terminal region of HSP90 ORF and a HindIII site in the vector (positions 3396 and 4807 regarding the sequence annotation of pcDNA3_HSP90_HA; note that the HSP90_HA ORF is located on the complementary strand) by a fragment that consisted of the same nucleotide sequence of the vector between the upstream Hind III site and the former start codon linked to Ypet, than the flexible linker and finally the HSP90 ORF from Gly-127 until the downstream HindIII site. Therefore, several PCRs were carried out using the KAPA HIFI polymerase (Roche, Switzerland) together with dNTPs and buffer according to the manufacturer's recommendations and 0.75 pmoles of each primer. 50 ng of plasmid DNA was used as a template in the initial PCR reactions. Later, when two PCR products were combined to longer single amplicons, usually 0.5 μl of the purified PCR products from the previous reactions were added as a template. Typical cycling conditions were: 35 cycles of denaturing (98 °C for 20 s), annealing (56–60 °C for 15 s); and elongation (72 °C for 60–90 s). The detailed procedure and primer sequences are described in S3 section. Expected protein molecular weights from each plasmid overexpression can be found in S4 section.

4.10. Statistical analysis

Statistical analyses were performed using the Prism 5 software (Graph-Pad, La Jolla, CA, USA). Most of the experiments were carried out at least as three independent experiments and are presented as mean values ± SD. Student's *t*-test was used to compare two groups. p value of < 0.05 was accepted as statistically significant.

CRediT authorship contribution statement

José Pedro Castro: Conceptualization, Investigation, Writing - original draft, Writing - review & editing. **Raquel Fernando:** Investigation. **Sandra Reeg:** Investigation. **Walter Meinl:** Investigation. **Henrique Almeida:** Conceptualization, Writing - original draft, Writing - review & editing. **Tilman Grune:** Conceptualization, Writing - original draft, Writing - review & editing.

Acknowledgements

TG was supported by DFG and the 'Gesundheitscampus Brandenburg'. JPC got a short term travel fellowship from DAAD.

Conflict of interest

None.

Funding

This work was in part funded by the German Research Foundation (DFG).

Appendix A. Supporting information

Supplementary data associated with this article can be found in the online version at doi:10.1016/j.redox.2019.101108

References

[1] T.B. Kirkwood, S.N. Austad, Why do we age? Nature 408 (6809) (2000) 233–238.
[2] T.B. Kirkwood, Understanding the odd science of aging, Cell 120 (4) (2005) 437–447.
[3] V.N. Gladyshev, Aging: progressive decline in fitness due to the rising deleteriome adjusted by genetic, environmental, and stochastic processes, Aging Cell 15 (4) (2016) 594–602.
[4] R.L. Levine, E.R. Stadtman, Oxidative modification of proteins during aging, Exp. Gerontol. 36 (9) (2001) 1495–1502.
[5] T. Nystrom, Role of oxidative carbonylation in protein quality control and senescence, EMBO J. 24 (7) (2005) 1311–1317.
[6] T. Grune, T. Reinheckel, K.J. Davies, Degradation of oxidized proteins in mammalian cells, FASEB J. 11 (7) (1997) 526–534.
[7] T. Grune, T. Reinheckel, M. Joshi, K.J.A. Davies, Proteolysis in cultured Liver epithelial cells during oxidative stress: role of the multicatalytic proteinase complex, proteasome, J. Biol. Chem. 270 (5) (1995) 2344–2351.
[8] T. Grune, T. Reinheckel, K.J.A. Davies, Degradation of oxidized proteins in K562 human hematopoietic cells by proteasome, J. Biol. Chem. 271 (26) (1996) 15504–15509.
[9] T. Jung, B. Catalgol, T. Grune, The proteasomal system, Mol. Asp. Med. 30 (4) (2009) 191–296.
[10] O. Ullrich, et al., Poly-ADP ribose polymerase activates nuclear proteasome to degrade oxidatively damaged histones, Proc. Natl. Acad. Sci. 96 (11) (1999) 6223–6228.
[11] M. Kästle, T. Grune, Proteins bearing oxidation-induced carbonyl groups are not preferentially ubiquitinated, Biochimie 93 (6) (2011) 1076–1079.
[12] M. Kästle, S. Reeg, A. Rogowska-Wrzesinska, T. Grune, Chaperones, but not oxidized proteins, are ubiquitinated after oxidative stress, Free Radic. Biol. Med. 53 (7) (2012) 1468–1477.
[13] T. Jung, T. Grune, The proteasome and the degradation of oxidized proteins: Part I-structure of proteasomes, Redox Biol. 1 (1) (2013) 178–182.
[14] N.F. Bence, R.M. Sampat, R.R. Kopito, Impairment of the ubiquitin-proteasome system by protein aggregation, Science 292 (5521) (2001) 1552–1555.
[15] N. Sitte, K. Merker, T. Von Zglinicki, T. Grune, K.J. Davies, Protein oxidation and degradation during cellular senescence of human BJ fibroblasts: part I–effects of proliferative senescence, FASEB J.: Off. Publ. Fed. Am. Soc. Exp. Biol. 14 (15) (2000) 2495–2502.
[16] N. SITTE, et al., Proteasome inhibition by lipofuscin/ceroid during postmitotic aging of fibroblasts, FASEB J. 14 (11) (2000) 1490–1498.
[17] T. Grune, T. Jung, K. Merker, K.J.A. Davies, Decreased proteolysis caused by protein aggregates, inclusion bodies, plaques, lipofuscin, ceroid, and 'aggresomes' during oxidative stress, aging, and disease, Int. J. Biochem. Cell Biol. 36 (12) (2004) 2519–2530.
[18] J.P. Castro, T. Jung, T. Grune, H. Almeida Actin carbonylation: From cell dysfunction to organism disorder, J. Proteom.
[19] S. Reeg, et al., The molecular chaperone Hsp70 promotes the proteolytic removal of oxidatively damaged proteins by the proteasome, Free Radic. Biol. Med. 99 (2016) 153–166.
[20] J.E. Whittier, Y. Xiong, M.C. Rechsteiner, T.C. Squier, Hsp90 enhances degradation of oxidized calmodulin by the 20 S proteasome, J. Biol. Chem. 279 (44) (2004) 46135–46142.
[21] M. Taipale, D.F. Jarosz, S. Lindquist, HSP90 at the hub of protein homeostasis: emerging mechanistic insights, Nat. Rev. Mol. Cell Biol. 11 (7) (2010) 515–528.
[22] W.B. Pratt, Y. Morishima, H.M. Peng, Y. Osawa, Proposal for a role of the Hsp90/Hsp70-based chaperone machinery in making triage decisions when proteins undergo oxidative and toxic damage, Exp. Biol. Med. 235 (3) (2010) 278–289.
[23] X. Lu, C. Michaud, M. Orlowski, Heat shock protein-90 and the catalytic activities of the 20 S proteasome (multicatalytic proteinase complex), Arch. Biochem. Biophys. 387 (1) (2001) 163–171.
[24] A.M. Eleuteri, et al., Interaction of Hsp90 with 20S proteasome: thermodynamic and kinetic characterization, Proteins 48 (2) (2002) 169–177.
[25] M. Conconi, L.I. Szweda, R.L. Levine, E.R. Stadtman, B. Friguet, Age-related decline of rat liver multicatalytic proteinase activity and protection from oxidative inactivation by heat-shock protein 90, Arch. Biochem. Biophys. 331 (2) (1996) 232–240.
[26] M. Conconi, et al., Protection from oxidative inactivation of the 20S proteasome by heat-shock protein 90, Biochem. J. 333 (Pt 2) (1998) 407–415.
[27] J.P. Castro, C. Ott, T. Jung, T. Grune, H. Almeida, Carbonylation of the cytoskeletal protein actin leads to aggregate formation, Free Radic. Biol. Med. 53 (4) (2012) 916–925.
[28] R. Das, S. Ponnappan, U. Ponnappan, Redox regulation of the proteasome in T lymphocytes during aging, Free Radic. Biol. Med. 42 (4) (2007) 541–551.
[29] U. Ponnappan, M. Zhong, G.U. Trebilcock, Decreased proteasome-mediated degradation in T cells from the elderly: a role in immune senescence, Cell. Immunol. 192 (2) (1999) 167–174.
[30] L.-M. Gerland, et al., Autolysosomes accumulate during in vitro CD8+ T-lymphocyte aging and may participate in induced death sensitization of senescent cells, Exp. Gerontol. 39 (5) (2004) 789–800.
[31] S. Koyasu, et al., Two mammalian heat shock proteins, HSP90 and HSP100, are actin-binding proteins, Proc. Natl. Acad. Sci. 83 (21) (1986) 8054–8058.
[32] S.J. Park, S. Suetsugu, H. Sagara, T. Takenawa, HSP90 cross-links branched actin filaments induced by N-WASP and the Arp2/3 complex, Genes Cells 12 (5) (2007) 611–622.
[33] A. Taiyab, C.M. Rao, HSP90 modulates actin dynamics: inhibition of HSP90 leads to decreased cell motility and impairs invasion, Biochim. Biophys. Acta (BBA) - Mol. Cell Res. 1813 (1) (2011) 213–221.
[34] E. Nishida, S. Koyasu, H. Sakai, I. Yahara, Calmodulin-regulated binding of the 90-kDa heat shock protein to actin filaments, J. Biol. Chem. 261 (34) (1986) 16033–16036.
[35] Y. Miyata, I. Yahara, Cytoplasmic 8 S glucocorticoid receptor binds to actin filaments through the 90-kDa heat shock protein moiety, J. Biol. Chem. 266 (14) (1991) 8779–8783.
[36] M.S.Z. Kellermayer, P. Csermely, ATP induces dissociation of the 90-kDa heat shock protein (hsp90) from F-actin: interference with the binding of heavy meromyosin, Biochem. Biophys. Res. Commun. 211 (1) (1995) 166–174.
[37] P.A. Tsaytler, J. Krijgsveld, S.S. Goerdayal, S. Rudiger, M.R. Egmond, Novel Hsp90 partners discovered using complementary proteomic approaches, Cell Stress Chaperon-. 14 (6) (2009) 629–638.
[38] G. Hild, B. Bugyi, M. Nyitrai, Conformational dynamics of actin: effectors and implications for biological function, Cytoskeleton 67 (10) (2010) 609–629.
[39] M. Fujimoto, A. Nakai, The heat shock factor family and adaptation to proteotoxic stress, FEBS J. 277 (20) (2010) 4112–4125.
[40] A. Zuehlke, J.L. Johnson, Hsp90 and co-chaperones twist the functions of diverse client proteins, Biopolymers 93 (3) (2010) 211–217.
[41] A.J. McClellan, S. Tam, D. Kaganovich, J. Frydman, Protein quality control: chaperones culling corrupt conformations, Nat. Cell Biol. 7 (8) (2005) 736–741.
[42] E.R. Stadtman, R.L. Levine, Protein oxidation, Ann. N.Y. Acad. Sci. 899 (1) (2000) 191–208.
[43] R. Beck, et al., Hsp90 is cleaved by reactive oxygen species at a highly conserved N-terminal amino acid motif, PLoS One 7 (7) (2012) e40795.
[44] D. Trachootham, J. Alexandre, P. Huang, Targeting cancer cells by ROS-mediated mechanisms: a radical therapeutic approach? Nat. Rev. Drug Discov. 8 (7) (2009) 579–591.
[45] G.T. Wondrak, Redox-directed cancer therapeutics: molecular mechanisms and opportunities, Antioxid. Redox Signal. 11 (12) (2009) 3013–3069.
[46] X. Ye, et al., Cytotoxic effects of Mn(III) N-alkylpyridylporphyrins in the presence of cellular reductant, ascorbate, Free Radic. Res. 45 (11–12) (2011) 1289–1306.
[47] G. Garcia-Cardena, et al., Dynamic activation of endothelial nitric oxide synthase by Hsp90, Nature 392 (6678) (1998) 821–824.
[48] K. Nowotny, T. Jung, T. Grune, A. Hohn, Accumulation of modified proteins and aggregate formation in aging, Exp. Gerontol. 57C (2014) 122–131.
[49] A. Höhn, T. Jung, T. Grune Pathophysiological importance of aggregated damaged proteins, Free Radic. Biol. Med.
[50] A.B. Lindner, R. Madden, A. Demarez, E.J. Stewart, F. Taddei, Asymmetric segregation of protein aggregates is associated with cellular aging and rejuvenation, Proc. Natl. Acad. Sci. 105 (8) (2008) 3076–3081.
[51] S. Dukan, T. Nystrom, Bacterial senescence: stasis results in increased and differential oxidation of cytoplasmic proteins leading to developmental induction of the heat shock regulon, Genes Dev. 12 (21) (1998) 3431–3441.
[52] H. Mirzaei, F. Regnier, Identification of yeast oxidized proteins: chromatographic top-down approach for identification of carbonylated, fragmented and cross-linked proteins in yeast, J. Chromatogr. A 1141 (1) (2007) 22–31.
[53] D.C. David, et al., Widespread protein aggregation as an inherent part of aging in C. elegans, PLoS Biol. 8 (8) (2010) e1000450.
[54] N. Sitte, et al., Proteasome inhibition by lipofuscin/ceroid during postmitotic aging of fibroblasts, FASEB J.: Off. Publ. Fed. Am. Soc. Exp. Biol. 14 (11) (2000) 1490–1498.
[55] T. Grune, K. Merker, G. Sandig, K.J.A. Davies, Selective degradation of oxidatively modified protein substrates by the proteasome, Biochem. Biophys. Res. Commun. 305 (3) (2003) 709–718.
[56] C.T. Aiken, R.M. Kaake, X. Wang, L. Huang, Oxidative stress-mediated regulation of proteasome complexes, Mol. Cell. Proteom.: MCP 10 (5) (2011) R110 (006924).
[57] M. Strosova, P. Voss, M. Engels, L. Horakova, T. Grune, Limited degradation of oxidized calmodulin by proteasome: formation of peptides, Arch. Biochem. Biophys. 475 (1) (2008) 50–54.
[58] I. Lassing, et al., Molecular and structural basis for redox regulation of β-actin, J. Mol. Biol. 370 (2) (2007) 331–348.
[59] I. Dalle-Donne, et al., Methionine oxidation as a major cause of the functional impairment of oxidized actin, Free Radic. Biol. Med. 32 (9) (2002) 927–937.
[60] P.C. Burcham, A. Raso, L.M. Kaminskas, Chaperone heat shock protein 90 mobilization and hydralazine cytoprotection against acrolein-induced carbonyl stress, Mol. Pharmacol. 82 (5) (2012) 876–886.
[61] K.J. Davies, Protein damage and degradation by oxygen radicals. I. general aspects, J. Biol. Chem. 262 (20) (1987) 9895–9901.
[62] N. Chondrogianni, et al., Central role of the proteasome in senescence and survival of human fibroblasts: induction of a senescence-like phenotype upon its inhibition and resistance to stress upon its activation, J. Biol. Chem. 278 (30) (2003) 28026–28037.
[63] J. Egea, I. Fabregat, Y.M. Frapart, et al., European contribution to the study of ROS: a summary of the findings and prospects for the future from the COST action BM1203 (EU-ROS), Redox Biol. 13 (2017) 94–162.
[64] R. Fernando, C. Drescher, K. Nowotny, T. Grune, J.P. Castro, Impaired proteostasis during skeletal muscle aging, Free Radic. Biol. Med. (2018) (Epub ahead of print).
[65] A. Höhn, D. Weber, T. Jung, C. Ott, M. Hugo, B. Kochlik, R. Kehm, J. König, T. Grune, J.P. Castro, Happily (n)ever after: aging in the context of oxidative stress, proteostasis loss and cellular senescence, Redox Biol. 11 (2017) 482–501.
[66] M. Sevin, F. Girodon, C. Garrido, A. de Thonel, HSP90 and HSP70: implication in inflammation processes and therapeutic approaches for myeloproliferative neoplasms, Mediat. Inflamm. 2015 (2015) 970242.
[67] M.M. Bradford, A rapid and sensitive method for the quantitation of microgram

quantities of protein utilizing the principle of protein-dye binding, Anal. Biochem. 72 (1976) 248–254.
[68] E. Maisonneuve, L. Fraysse, S. Lignon, L. Capron, S. Dukan, Carbonylated proteins are detectable only in a degradation-resistant aggregate state in Escherichia coli, J. Bacteriol. 190 (20) (2008) 6609–6614.
[69] C. Ballestrem, B. Wehrle-Haller, B.A. Imhof, Actin dynamics in living mammalian cells, J. Cell Sci. 111 (Pt 12) (1998) 1649–1658.
[70] A.W. Nguyen, P.S. Daugherty, Evolutionary optimization of fluorescent proteins for intracellular FRET, Nat. Biotechnol. 23 (3) (2005) 355–360.